

带多充液圆柱贮箱航天器刚 – 液耦合动力学研究

吴文军^{1,2}, 岳宝增¹, 黄华³

(1. 北京理工大学宇航学院, 北京 100081; 2. 广西科技大学汽车与交通学院, 柳州 545006;
3. 中国空间技术研究院通信卫星事业部, 北京 100094)

摘要: 文中以在低重环境下带多充液圆柱贮箱刚性航天器中刚 – 液耦合方程的建立和求解为主要研究目的。推导航天器中充液圆柱贮箱内任意点的牵连运动方程, 根据壁面边界条件给出了贮箱内液体牵连晃动势的表达式; 利用第二类边界条件下的傅立叶 – 贝塞尔级数展开法对低重力环境下的弯曲自由液面处的复杂动力学边界条件进行处理, 建立以液体相对晃动势的模态坐标和晃动波高的模态坐标为状态向量的液体耦合晃动力学方程, 通过积分分别得到了耦合晃动力和耦合晃动力矩的解析式; 运用准坐标系下的拉格朗日方程建立以航天器主刚体姿态坐标和轨道坐标为状态向量的刚体耦合运动动力学方程, 进一步联立上述耦合方程得到航天器整体系统的刚 – 液耦合动力学状态方程; 最后, 编制出适用于带多充液圆柱贮箱航天器内刚 – 液耦合动力学计算的模块化计算程序, 通过计算实例验证所编程序的准确性的同时, 研究了携带多充液箱航天器系统贮箱布局、外激励方式对航天器刚 – 液耦合系统动力学特性的影响。

关键词: 低重力环境; 多充液圆柱贮箱; 刚 – 液耦合动力学; 傅立叶 – 贝塞尔级数; 模态坐标法

中图分类号: V219 **文献标识码:** A **文章编号:** 1000-1328(2015)06-0648-13

DOI: 10.3873/j.issn.1000-1328.2015.06.005

Study on the Rigid-Liquid Coupled Dynamics for Spacecraft with Multiple Partially Liquid-filled Cylindrical Tanks

WU Wen-jun^{1,2}, YUE Bao-zeng¹, HUANG Hua³

(1. School of Aerospace Engineering, Beijing Institute of Technology, Beijing 100081, China;
2. School of Automobile and Traffic Engineering, Guangxi University of Science and Technology, Liuzhou 545006, China;
3. Satellite Communication Department, China Academy of Space Technology, Beijing 100094, China)

Abstract: In this paper, the solution and model of rigid-liquid coupled dynamics state equations of spacecraft with multiple liquid-filled cylindrical tanks in low-gravity environment are mainly studied. Firstly, the carrier motions equations of a representative point in liquid-filled cylindrical tank in spacecraft are deduced, and the carrier potential function equations of liquid in the tank are given according to wall boundary conditions. The complex dynamic boundaries conditions on curved free-surface under low-gravity environment are transformed to general simple differential equations by means of Fourier-Bessel series expansion method. The dynamic state equations for coupled rigid-liquid spacecraft system are presented, in which, the state vectors of equations consist of the modal coordinates of relative potential function and the modal coordinates of wave height. The formulas of coupled sloshing forces and coupled sloshing moments are obtained by integrating. Then the dynamic state equations of coupled motion of main body are deduced using the Lagrange's equations in terms of general quasi-coordinates. Correspondingly, the rigid-liquid coupled dynamics state equations of whole systems of spacecraft are obtained. Lastly, a modularized calculation code based on the present method is programmed. The influences of layouts of multi-tanks and driving mode on the dynamics performance of coupled rigid-liquid system are studied. Consequently, the validity of the presented methods and the computer program are verified.

Key words: Low-gravity environment; Multiple-liquid-filled cylindrical tanks; Rigid-liquid coupled dynamics; Fourier-Bessel series; Modal coordinate method

0 引言

要完成长时间及复杂的飞行任务, 现代大型航天器需要携带更多的发动机液体燃料(其质量占航天器整体质量的比例甚至会高达 60% 以上)。自二十世纪 70 年代以来对充液航天器中刚 - 液耦合、刚 - 液 - 柔耦合、刚 - 液 - 控耦合等问题的研究一直都备受国内外相关学者们的高度关注。另外, 随着贮箱几何尺寸的增大, 贮箱内液体晃动的固有频率会明显降低; 尤其在低重力环境下($10 \leqslant \text{Bond} \leqslant 100$), 液体晃动的固有频率与航天器中携带的大型柔性附件振动的固有频率更加相近, 以至于诱发低频共振而引发航天器姿态失稳; 现代航天器的设计过程中多采用多个并联或串联的小尺寸贮箱来代替单个大尺寸贮箱用于存贮所需的液体燃料。由于在多贮箱的液体晃动问题中涉及到贮箱位置布局的优化、不同贮箱间因燃料消耗量不均引发的不平衡、晃动固有频率相近的不同贮箱内产生的共振或拍振晃动等复杂动力学问题, 总体设计上的任何微小偏差均将直接影响航天器中姿态稳定与控制系统的执行效率和效果; 因此, 对带多充液贮箱航天器内液体晃动问题的研究比对带单贮箱航天器的情形相比将更复杂、更具挑战性和更具有工程应用价值。

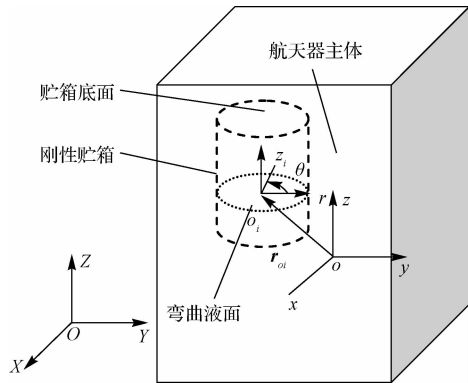
目前国内外已有不少文献报道了运用解析法、数值法或实验法对带单充液贮箱航天器刚 - 液耦合动力学问题的相关研究成果^[1-7]; 此外, 在对采用等效力学模型这一传统方法研究液体晃动动力学方面, 在对带单贮箱及多贮箱航天器耦合动力学与控制问题的研究也取得了大量卓有成效的研究成果^[8-14]。然而, 采用等效力学模型方法不能真实描述带多充液贮箱航天器耦合系统中多模态、内共振等耦合动力学现象以及其它更为复杂的刚 - 液耦合动力学特性。

本文将在此前研究工作的基础上, 以液体晃动力和晃动力矩为耦合内力传递项建立带多个圆柱贮箱刚体航天器的刚 - 液耦合动力学状态方程, 其中状态向量直接由液体晃动模态坐标和航天器主体姿态、轨道坐标组成。这不仅无需采用等效力学模型

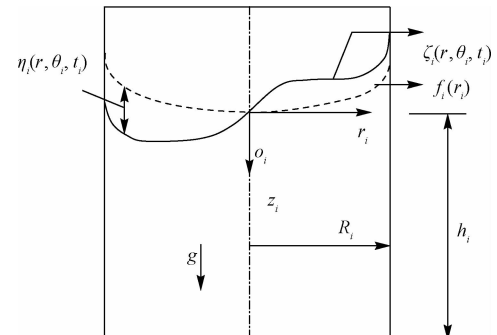
替代液体晃动, 而且依本文方法所编制的计算机仿真模块化程序将更便于进一步对带任意数目的多充液圆柱贮箱复杂航天器刚 - 液耦合动力学仿真计算问题进行全面、深入和细致的研究; 从而将有助于对现代复杂航天器更进一步开展刚 - 液 - 柔 - 控耦合动力学研究。

1 耦合动力方程的推导与求解

1.1 坐标系的建立



(a) 航天器的整体坐标系
(a) Global coordinate system of spacecraft



(b) 圆柱腔的局部坐标系
(b) Local coordinate system of cylindrical tank

图 1 航天器系统的坐标系

Fig. 1 Coordinate of spacecraft system

以携带单个圆柱贮箱的航天器为例, 假设充液柱箱相对于航天器主体固定, 航天器系统的坐标系如图 1 所示。图中, $OXYZ$ 为空间惯性直角坐标系(简称为惯性坐标系, Z 轴正向指向地心, X 轴为航天器轨道的正切线); $oxyz$ 为航天器主体的随体直角坐标系(简称为主体坐标系), 其与航天器主体的

主惯性轴一致。在第 i 个贮箱中: $f_i(r_i)$ 为静液面形
状; $\zeta_i(r_i, \theta_i, t_i)$ 为液面总波高函数; $\eta_i(r_i, \theta_i, t)$ 为
液面晃动波高函数; R_i 为贮箱的内半径; h_i 为的静
液面中心至贮箱底面的深度; 贮箱的局部柱坐标系
 $o_i r_i \theta_i z_i$ 和角坐标系 $o_i x_i y_i z_i$ 的坐标原点取为弯曲静液面
的中心点, 并设定 $o_i x_i y_i z_i$ 与 $oxyz$ 矢量方向保持一
致, 则两坐标轴间的转换矩阵为单位矩阵, $\mathbf{r}_{oi} =$
 $[r_{xi}, r_{yi}, r_{zi}]^T$ 为贮箱随体坐标系的原点坐标在 $oxyz$
坐标系下的矢径。设航天器主体在主体坐标系下的
速度向量和角速度向量分别为 $\mathbf{v} = [v_x, v_y, v_z]^T$ 和 $\boldsymbol{\omega}$
 $= [\omega_x, \omega_y, \omega_z]^T$ 。

为书写方便, 分别记圆柱贮箱侧壁面处边界面为 \mathbf{W}_i (即当 $r_i = R_i$ 时)、圆柱贮箱平底面处边界面为 \mathbf{B}_i (即当 $z_i = h_i$ 时,)、自由弯曲液面处边界面为 \mathbf{S}_i (即当 $z_i = -\zeta_i$ 时)、自由液面与贮箱壁面的边界线为 \mathbf{L}_i (即当 $r_i = R_i$ 且 $z_i = -\zeta_i$ 时)。

1.2 牵连速度势的推导

贮箱内任意点 p 的速度为

$$\mathbf{v}_p = \mathbf{v} + \mathbf{r}_p^\times \boldsymbol{\omega} \quad (1)$$

式中: $(\cdot)^\times$ 为矢量叉乘矩阵符; \mathbf{r}_p 为贮箱内任意点 p 在随体坐标系下的矢径。

依式(1)、直角坐标与柱坐标间的转换关系, 易得经整理后的贮箱内任意点在 $o_i r_i \theta_i z_i$ 下的速度为

$$\begin{cases} v_r = [v_x - \omega_z r_{yi} + \omega_y (r_{zi} + z_i)] \cos\theta + \\ \quad [v_y + \omega_z r_{xi} - \omega_x (r_{zi} + z_i)] \sin\theta \\ v_\theta = -[v_x - \omega_z r_{yi} + \omega_y (r_{zi} + z_i)] \sin\theta + \\ \quad [v_y + \omega_z r_{xi} - \omega_x (r_{zi} + z_i)] \cos\theta + \omega_z r \\ v_z = v_z + \omega_x r_{yi} - \omega_y r_{xi} + \omega_x r \sin\theta - \omega_y r \cos\theta \end{cases} \quad (2)$$

由式(2)可知, 在该类坐标体系下贮箱内任意点在 $o_i r_i \theta_i z_i$ 下的径向速度与 r_i 的值无关; 贮箱内任意点在 $o_i r_i \theta_i z_i$ 下的沿 z_i 轴方向的速度与 z_i 的值无关。另外, 依据理想流体为无黏、无旋的假设, 可忽略 v_θ 对贮箱内液体晃动的影响。

依文献 [15–16] 可知, 在小幅晃动范围内, 不论贮箱承受何种形式的运动激励, 贮箱的液体晃动速度势均可以通过叠加原理分解为牵连晃动速度势和相对晃动速度势。其中, 牵连速度势应完全满足的所有非齐次壁面边界条件, 依据液体的假设条件, 可得第 i 个贮箱内的牵连速度势 Φ_e 应满足的基本

方程为

$$\nabla^2 \Phi_e = 0 \quad (3)$$

$$\mathbf{W}_i: \frac{\partial \Phi_e}{\partial R} = \bar{v}_{ri} \quad (4)$$

$$\mathbf{B}_i: \frac{\partial \Phi_e}{\partial Z} = \bar{v}_{zi} \quad (5)$$

式中: $\Phi_e = \varphi_e / R_i^2$; $Z = z_i / R_i$; $R = r_i / R_i$; $H_i = h_i / R_i$; $\bar{v}_{ri} = (v_{ri}|_{R=1}) / R_i$; $\bar{v}_{zi} = (v_{zi}|_{Z=-H_i}) / R_i$; φ_e 为牵连晃动速度势。为书写方便, 本文中已将贮箱内局部坐标的下标省略。

显然, 可将 Φ_e 分解为 Φ_{e1} 和 Φ_{e2} , 并令 Φ_{e1} 同时满足式(3)、(4), 则可设

$$\Phi_{e1} = (\bar{v}_r|_{R=1}) R \quad (6)$$

将式(6)代入式(4)、(5)后, 经整理可得

$$\mathbf{W}_i: \frac{\partial \Phi_{e2}}{\partial R} = 0 \quad (7)$$

$$\mathbf{B}_i: \frac{\partial \Phi_{e2}}{\partial Z} = \bar{v}_z + \omega_x R_{yi} - \omega_y R_{xi} + 2\omega_x R \sin\theta - 2\omega_y R \cos\theta \quad (8)$$

式中: $\bar{v}_z = V_z / Rt$ 为使 φ_{e2} 同时满足式(3)、(7)和(8), 可设

$$\Phi_{e2} = (\bar{v}_z + \omega_x R_{yi} - \omega_y R_{xi}) Z + \sum_{n=1}^{\infty} \left[A_n(t) \frac{\sinh(\lambda_{n1} Z)}{\cosh(\lambda_{n1} H_i)} J_1(\lambda_{n1} R) \sin\theta + B_n(t) \frac{\sinh(\lambda_{n1} Z)}{\cosh(\lambda_{n1} H_i)} J_1(\lambda_{n1} R) \cos\theta \right] \quad (9)$$

式中: λ_{n1} 为方程 $J_1'(\lambda_n) = 0$ 的根; $H_i = h_i / R_i$; $n = 1, 2, \dots, N$; N 为径向模态最大展开项数。利用第二类边界条件下的傅立叶-贝塞尔级数展开法对式(8)中的参数 R 进行展开后, 利用贝塞尔函数的正交性, 经比较对应项系数后, 易得

$$A_n(t) = \frac{4\omega_x}{\lambda_{n1}(\lambda_{n1}^2 - 1)J_1(\lambda_{n1})} \quad (10)$$

$$B_n(t) = -\frac{4\omega_y}{\lambda_{n1}(\lambda_{n1}^2 - 1)J_1(\lambda_{n1})} \quad (11)$$

联立式(2)、(6)和(9)~(11)后, 可得

$$\begin{aligned} \Phi_e = & \{[\bar{v}_x - \omega_z R_{yi} + \omega_y (R_{zi} + Z)] \cos\theta + \\ & [\bar{v}_y + \omega_z R_{xi} - \omega_x (R_{zi} + Z)] \sin\theta\} R + \\ & (\bar{v}_z + \omega_x R_{yi} - \omega_y R_{xi}) Z + \\ & \sum_{n=1}^{\infty} \left[\frac{4\omega_x}{\lambda_{n1}(\lambda_{n1}^2 - 1)J_1(\lambda_{n1})} \frac{\sinh(\lambda_{n1} Z)}{\cosh(\lambda_{n1} H_i)} \right. \end{aligned}$$

$$J_1(\lambda_{n1}R)\sin\theta - \frac{4\omega_y}{\lambda_{n1}(\lambda_{n1}^2 - 1)J_1(\lambda_{n1})} \cdot \\ \left. \frac{\sinh(\lambda_{n1}Z)}{\cosh(\lambda_{n1}H_i)} J_1(\lambda_{n1}R)\cos\theta \right] \quad (12)$$

式中: $\bar{v}_x = V_x/Rt$; $\bar{v}_y = V_y/Rt$ 显然, 式(12)已自然完全满足式(3)~(5)。

1.3 液体晃动的模态坐标

相对晃动速度势 Φ_r 除需满足式(3)~(5)的齐次形式外, 还需满足自由液面处的动边界条件。在小幅晃动情况下, 其可简化为

$$S_i: \frac{\partial\psi}{\partial t} - \frac{\partial(\Phi_r + \Phi_e)}{\partial Z} + \frac{\partial(\Phi_r + \Phi_e)}{\partial R} \frac{dF(R)}{dR} = 0 \quad (13)$$

$$S_i: \frac{\partial(\Phi_r + \Phi_e)}{\partial t} + \frac{g}{R_i}\psi - \frac{\sigma_i}{R_i^3} \left\{ \frac{1}{R} \frac{\partial}{\partial R} \left\{ \frac{R \frac{\partial\psi}{\partial R}}{\left[1 + \left(\frac{dF(R)}{dR} \right)^2 \right]^{\frac{3}{2}}} \right\} + \frac{1}{R^2} \frac{\partial}{\partial\theta} \left\{ \frac{\frac{\partial\psi}{\partial\theta}}{\left[1 + \left(\frac{dF(R)}{dR} \right)^2 \right]^{\frac{1}{2}}} \right\} \right\} = 0 \quad (14)$$

式中: $\psi = \eta_i/R_i$; $F(R) = f_i(r_i)/R_i$

另外, 相对晃动波高 ψ 除满足式(13)、(14)外, 还需满足自由接触线条件

$$L_i: \frac{\partial\psi}{\partial R} = 0 \quad (15)$$

对于满足拉普拉斯方程和齐次壁面边界条件的相对晃动速度势 Φ_r 、相对晃动波高 ψ 的表达式可分别设为

$$\Phi_r(R, \theta, Z, t) = \sum_{n=1}^{\infty} \sum_{m=0}^{\infty} [a_{nm}(t) \cos(m\theta) + b_{nm}(t) \sin(m\theta)] J_m(\lambda_{nm}R) \frac{\cosh[\lambda_{nm}(Z - H_i)]}{\cosh(\lambda_{nm}H_i)} \quad (16)$$

$$\psi(R, \theta, t) = \sum_{n=1}^{\infty} \sum_{m=0}^{\infty} [c_{nm}(t) \cos(m\theta) + d_{nm}(t) \sin(m\theta)] J_m(\lambda_{nm}R) \quad (17)$$

式中: λ_{nm} 为方程 $J_m'(\lambda_n) = 0$ 的根; $m = 0, 1, 2, \dots, M$; M 为周向模态最大展开项数。

1.4 晃动力和晃动力矩

一般情况下, 液体晃动系统晃动稳态解的占优

晃动模态仅与牵连晃动速度势有关, 而牵连晃动速度势的形式由航天器主体的姿、轨坐标确定, 反之, 由于液体晃动产生的不平衡力又影响航天器主体的姿、轨坐标, 故该液体晃动系统为典型的耦合系统。依圆柱贮箱几何尺寸的规则性, 下一步从晃动力和晃动力矩的解析式来分析该类航天器中刚液耦合系统的占优晃动模态。

沿 x_i 、 y_i 和 z_i 轴方向的晃动力由液面与壁面接触线处的表面张力和液体内动压强引起, 其形式分别为

$$F_{xi}(t) = - \int_0^{2\pi} \left(\frac{\partial\eta}{\partial\theta} \Big|_{r=R_i} \right) \sigma_i \sin\theta d\theta + \int_0^{2\pi} \int_{-\xi_i}^{h_i} (P \Big|_{r=R_i}) R_i \cos\theta dz d\theta \quad (18)$$

$$F_{yi}(t) = - \int_0^{2\pi} \left(\frac{\partial\eta}{\partial\theta} \Big|_{r=R_i} \right) \sigma_i \cos\theta d\theta + \int_0^{2\pi} \int_{-\xi_i}^{h_i} (P \Big|_{r=R_i}) R_i \sin\theta dz d\theta \quad (19)$$

$$F_{zi}(t) = \int_0^{2\pi} \int_0^{R_i} (P \Big|_{z=h_i}) r d\theta dr \quad (20)$$

将式(12)、(16)和(17)分别代入式(18)、(19)、(20), 并积分后分别可得

$$F_{xi}(t) = -\rho_i \pi R_i^5 \left\{ [\dot{v}_x - \dot{\omega}_z R_{yi} + \dot{\omega}_y R_{zi}] (\beta_i + H_i) + \dot{\omega}_y \frac{1}{2} (H_i^2 - \beta_i^2) \right\} + \pi R_i \sigma_i \left[\sum_{n=1}^{\infty} c_{n1}(t) J_1(\lambda_{n1}) \right] + \rho_i \pi \beta_i R_i^4 (\dot{v}_z + \dot{\omega}_x R_{yi} - \dot{\omega}_y R_{xi}) \left[\sum_{n=1}^{\infty} c_{n1}(t) J_1(\lambda_{n1}) \right] + \rho_i \pi R_i^4 \sum_{n=1}^{\infty} \frac{4\dot{\omega}_y}{\lambda_{n1}^2 (\lambda_{n1}^2 - 1)} \cdot \frac{\sinh[\lambda_{n1}(\beta_i + H_i)]}{\cosh(\lambda_{n1}H_i)} - \rho_i \pi R_i^4 \sum_{n=1}^{\infty} \dot{a}_{n1}(t) J_1(\lambda_{n1}) \cdot \frac{\sinh[\lambda_{n1}(\beta_i + H_i)]}{\lambda_{n1} \cosh(\lambda_{n1}H_i)} \quad (21)$$

$$F_{yi}(t) = -\rho_i \pi R_i^5 \left\{ [\dot{v}_y + \dot{\omega}_z R_{xi} - \dot{\omega}_x R_{zi}] \right\} \cdot$$

$$\begin{aligned}
& \left. (\beta_i + H_i) + \dot{\omega}_x \frac{1}{2} (H_i^2 - \beta_i^2) \right\} + \\
& \pi R_i \sigma_i \left[\sum_{n=1}^{\infty} d_{n1}(t) J_1(\lambda_{n1}) \right] - \\
& \rho_i \pi \beta_i R_i^4 \left(\dot{v}_z + \dot{\omega}_x R_{yi} - \dot{\omega}_y R_{xi} \right) \left[\sum_{n=1}^{\infty} d_{n1}(t) J_1(\lambda_{n1}) \right] - \\
& \rho_i \pi R_i^4 \sum_{n=1}^{\infty} \frac{4\dot{\omega}_x}{\lambda_{n1}^2 (\lambda_{n1}^2 - 1)} \cdot \\
& \frac{\sinh[\lambda_{n1}(\beta_i + H_i)]}{\cosh(\lambda_{n1}H_i)} + \\
& \rho_i \pi R_i^4 \sum_{n=1}^{\infty} b_{n1}(t) J_1(\lambda_{n1}) \cdot \\
& \frac{\sinh[\lambda_{n1}(\beta_i + H_i)]}{\lambda_{n1} \cosh(\lambda_{n1}H_i)} \quad (22)
\end{aligned}$$

$$\begin{aligned}
F_{zi}(t) = & -\rho_i \pi R_i^3 H_i \left(\dot{v}_z + \dot{\omega}_x R_{yi} - \dot{\omega}_y R_{xi} \right) - \\
& 2\rho_i \pi R_i^2 \int_0^{R_i} \left(\sum_{n=1}^{\infty} \dot{a}_{n0}(t) \frac{J_0(\lambda_{n0}r/R_i)}{\cosh(\lambda_{n0}H_i)} \right) r dr \quad (23)
\end{aligned}$$

同理, 液体晃动对 $o_i x_i y_i z_i$ 中各轴产生的晃动力矩的表达式分别为

$$\begin{aligned}
M_{xi}(t) = & - \int_0^{2\pi} (\beta_i R_i + \eta|_{r=R_i}) \left(\frac{\partial \eta}{\partial \theta} \Big|_{r=R_i} \right) \sigma \cos \theta d\theta - \\
& \int_0^{2\pi} \int_{-\xi_i}^h (P|_{r=R_i}) z R_i \sin \theta dz d\theta + \\
& \int_0^{2\pi} \int_0^{R_i} (P|_{z=h_i}) r^2 \sin \theta d\theta dr \quad (24)
\end{aligned}$$

$$\begin{aligned}
M_{yi}(t) = & \int_0^{2\pi} (\beta_i R_i + \eta|_{r=R_i}) \left(\frac{\partial \eta}{\partial \theta} \Big|_{r=R_i} \right) \sigma_i \sin \theta d\theta + \\
& \int_0^{2\pi} \int_{-\xi_i}^h (P|_{r=R_i}) z R_i \cos \theta dz d\theta - \\
& \int_0^{2\pi} \int_0^{R_i} (P|_{z=h_i}) r^2 \cos \theta dr \quad (25)
\end{aligned}$$

将式(12)、(16)和(17)分别代入式(24)、(25), 利用三角函数的正交性, 略去高阶微量后分别可得

$$\begin{aligned}
M_{xi}(t) = & \frac{1}{2} \rho_i \pi R_i^6 [\dot{v}_y + \dot{\omega}_z R_{xi} - \dot{\omega}_x R_{zi}] (H_i^2 - \beta_i^2) + \\
& \frac{1}{3} \rho_i \pi R_i^6 \dot{\omega}_x (H_i^3 + \beta_i^3) - \\
& \pi R_i^2 \sigma_i \beta_i \left[\sum_{n=1}^{\infty} d_{n1}(t) J_1(\lambda_{n1}) \right] + \\
& \rho_i \pi \beta_i^2 R_i^5 [\dot{v}_z + \dot{\omega}_x R_{yi} - \dot{\omega}_y R_{xi}]
\end{aligned}$$

$$\begin{aligned}
& \dot{\omega}_y R_{xi} \left[\sum_{n=1}^{\infty} d_{n1}(t) J_1(\lambda_{n1}) \right] + \\
& \rho_i \pi R_i^4 \left\{ \sum_{n=1}^{\infty} \frac{4\dot{\omega}_x}{\lambda_{n1}^3 (\lambda_{n1}^2 - 1) \cosh(\lambda_{n1}H_i)} \right. \\
& [\lambda_{n1} h_i \cosh(\lambda_{n1}H_i) + \lambda_{n1} \beta_i R_i \cosh(\lambda_{n1}\beta_i) \\
& - R_i \sinh(\lambda_{n1}\beta_i) - R_i \sinh(\lambda_{n1}H_i)] \left. \right\} - \\
& \rho_i \pi R_i^2 \left[\sum_{n=1}^{\infty} \frac{4\dot{\omega}_x}{\lambda_{n1} (\lambda_{n1}^2 - 1) J_1(\lambda_{n1})} \right. \\
& \frac{\sinh(\lambda_{n1}H_i)}{\cosh(\lambda_{n1}H_i)} \int_0^{R_i} J_1(\lambda_{n1}R) r^2 dr \left. \right] - \\
& \frac{1}{4} \rho_i \pi R_i^5 [\dot{v}_y + \dot{\omega}_z R_{xi} - \dot{\omega}_x (R_{zi} + H_i)] + \\
& \rho_i \pi R_i^5 \left\{ \sum_{n=1}^{\infty} \frac{b_{n1}(t) J_1(\lambda_{n1})}{\lambda_{n1}^2 \cosh(\lambda_{n1}H_i)} \right. \\
& \cosh(\lambda_{n1}(\beta_i + H_i)) + \\
& \lambda_{n1} \beta_i \sinh(\lambda_{n1}(\beta_i + H_i)) - 1 \left. \right\} - \\
& \rho_i \pi R_i^2 \int_0^R \left(\sum_{n=1}^{\infty} b_{n1}(t) \frac{J_1(\lambda_{n1}r/R_i)}{\cosh(\lambda_{n1}H_i)} \right) r^2 dr - \\
& \rho_i g \pi \beta_i^2 R_i^4 \left[\sum_{n=1}^{\infty} d_{n1}(t) J_1(\lambda_{n1}) \right] \quad (26)
\end{aligned}$$

$$\begin{aligned}
M_{yi}(t) = & -\frac{1}{2} \rho_i \pi R_i^6 [\dot{v}_x - \dot{\omega}_z R_{yi} + \dot{\omega}_y R_{zi}] \\
& (H_i^2 - \beta_i^2) - \frac{1}{3} \rho_i \pi R_i^6 \dot{\omega}_y (H_i^3 + \beta_i^3) - \\
& \pi R_i^2 \sigma_i \beta_i \left[\sum_{n=1}^{\infty} c_{n1}(t) J_1(\lambda_{n1}) \right] - \\
& \rho_i \pi \beta_i^2 R_i^5 [\dot{v}_z + \dot{\omega}_x R_{yi} - \dot{\omega}_y R_{xi}] \\
& \left[\sum_{n=1}^{\infty} c_{n1}(t) J_1(\lambda_{n1}) \right] + \rho_i \pi R_i^4 \\
& \left[\sum_{n=1}^{\infty} \frac{4\dot{\omega}_y}{\lambda_{n1}^3 (\lambda_{n1}^2 - 1) \cosh(\lambda_{n1}H_i)} \right. \\
& \lambda_{n1} h_i \cosh(\lambda_{n1}H_i) - \lambda_{n1} \beta_i R_i \cosh(\lambda_{n1}\beta_i) \\
& + R_i \sinh(\lambda_{n1}\beta_i) - R_i \sinh(\lambda_{n1}H_i) \left. \right] - \\
& \rho_i \pi R_i^2 \sum_{n=1}^{\infty} \left[\frac{4\dot{\omega}_y}{\lambda_{n1} (\lambda_{n1}^2 - 1) J_1(\lambda_{n1})} \right. \\
& \frac{\sinh(\lambda_{n1}H_i)}{\cosh(\lambda_{n1}H_i)} \int_0^R J_1(\lambda_{n1}R) r^2 dr \left. \right] + \\
& \frac{1}{4} \rho_i \pi R_i^5 [\dot{v}_x - \dot{\omega}_z R_{yi} + \dot{\omega}_y (R_{zi} + H_i)] -
\end{aligned}$$

$$\begin{aligned} & \rho_i \pi R_i^5 \left\{ \sum_{n=1}^{\infty} \frac{\dot{a}_{n1}(t) J_1(\lambda_{n1})}{\lambda_{n1}^2 \cosh(\lambda_{n1} H_i)} \right. \\ & \cosh[\lambda_{n1}(\beta_i + H_i)] + \\ & \left. \lambda_{n1} \beta_i \sinh[\lambda_{n1}(\beta_i + H_i)] - 1 \right\} + \\ & \rho_i \pi R_i^2 \int_0^R \left(\sum_{n=1}^{\infty} \dot{a}_{n1}(t) \frac{J_1(\lambda_{n1} r / R_i)}{\cosh(\lambda_{n1} H_i)} \right) r^2 dr \end{aligned} \quad (27)$$

由式(21)~(23)、(26)~(27)可知,对于如图1所示的光圆柱贮箱内的液体晃动,由于正弦或余弦函数正交性存在,导致仅有 $m = 0$ 和 1 的晃动模态产生晃动力和晃动力矩;故在进行刚-液耦合晃动计算时,可仅考虑如下晃动模态对耦合系统的影响。

$$\begin{aligned} \Phi_r(R, \theta, Z, t) = & \sum_{n=1}^{\infty} \left\{ a_{n0} J_0(\lambda_{n0} R) \right. \\ & \frac{\cosh[\lambda_{n0}(Z - H_i)]}{\cosh(\lambda_{n0} H_i)} + [a_{n1}(t) \cos \theta + \\ & b_{n1}(t) \sin \theta] J_1(\lambda_{n1} R) \\ & \left. \frac{\cosh[\lambda_{n1}(Z - H_i)]}{\cosh(\lambda_{n1} H_i)} \right\} \end{aligned} \quad (28)$$

$$\psi(R, \theta, t) = \sum_{n=1}^{\infty} \{ c_{n0}(t) J_1(\lambda_{n0} R) + [c_{n1}(t) \cos \theta + \\ d_{n1}(t) \sin \theta] J_1(\lambda_{n1} R) \}$$

但在实际工程中,航天器的燃料贮箱一般均设置有环向或纵向的档板用于抑制液体的晃动,其晃动势在周向上将可能不是严格的正弦或余弦分布,相应的晃动力和晃动力矩的形式将可能会更加复杂,这也是作者们有待进一步研究的问题之一。

1.5 动边界条件的傅立叶-贝塞尔级数展开

将式(16)~(17)代入式(13)后,由三角函数的正交性,通过比较三角函数各项对应的系数后,分别可得。

$$\begin{aligned} & \sum_{n=1}^{\infty} \left\{ \left(\dot{c}_{n0}(t) - a_{n0}(t) \frac{\lambda_{n0} \sinh[\lambda_{n0}(Z_i - H_i)]}{\cosh(\lambda_{n0} H_i)} \right) \right. \\ & J_0(\lambda_{n0} R) + a_{n0}(t) \frac{\cosh[\lambda_{n0}(Z_i - H_i)]}{\cosh(\lambda_{n0} H_i)} \\ & \left. [J_0(\lambda_{n0} R)]' \left(\frac{dF}{dR} \right) \right\} = \bar{v}_z + \omega_x R_{yi} - \omega_y R_{xi} \quad (30) \end{aligned}$$

$$\begin{aligned} & \sum_{n=1}^{\infty} \left\{ \left(\dot{d}_{n1}(t) - b_{n1}(t) \frac{\lambda_{n1} \sinh[\lambda_{n0}(Z_i - H_i)]}{\cosh(\lambda_{n1} H_i)} \right) \right. \\ & J_1(\lambda_{n1} R) + b_{n1}(t) \frac{\cosh[\lambda_{n0}(Z_i - H_i)]}{\cosh(\lambda_{n0} H_i)} \\ & [J_1(\lambda_{n1} R)]' \left(\frac{dF}{dR} \right) + \frac{4\omega_x}{\lambda_{n1}(\lambda_{n1}^2 - 1) J_1(\lambda_{n1})} \\ & \left. \frac{\sinh(\lambda_{n1} Z_i)}{\cosh(\lambda_{n1} H_i)} [J_1(\lambda_{n1} R)]' \left(\frac{dF}{dR} \right) \right\} - \\ & \frac{4\omega_x}{(\lambda_{n1}^2 - 1) J_1(\lambda_{n1})} \frac{\cosh(\lambda_{n1} Z_i)}{\cosh(\lambda_{n1} H_i)} J_1(\lambda_{n1} R) + \\ & \omega_x R = 0 \end{aligned} \quad (31)$$

$$\begin{aligned} & \sum_{n=1}^{\infty} \left\{ \left(\dot{a}_{n1}(t) - a_{n1}(t) \frac{\lambda_{n1} \sinh[\lambda_{n0}(Z_i - H_i)]}{\cosh(\lambda_{n1} H_i)} \right) \right. \\ & J_1(\lambda_{n1} R) + a_{n1}(t) \frac{\cosh[\lambda_{n0}(Z_i - H_i)]}{\cosh(\lambda_{n0} H_i)} \\ & [J_1(\lambda_{n1} R)]' \left(\frac{dF}{dR} \right) + \frac{4\omega_y}{(\lambda_{n1}^2 - 1) J_1(\lambda_{n1})} \\ & \frac{\cosh(\lambda_{n1} Z_i)}{\cosh(\lambda_{n1} H_i)} J_1(\lambda_{n1} R) - \omega_y R - \\ & \frac{4\omega_y}{\lambda_{n1}(\lambda_{n1}^2 - 1) J_1(\lambda_{n1})} \frac{\sinh(\lambda_{n1} Z_i)}{\cosh(\lambda_{n1} H_i)} \\ & \left. [J_1(\lambda_{n1} R)]' \left(\frac{dF}{dR} \right) \right\} = 0 \end{aligned} \quad (32)$$

同理,将式(16)~(17)代入式(14)后,通过比较三角函数对应项系数后分别可得

$$\begin{aligned} & \sum_{n=1}^{\infty} \left\{ \left(\dot{a}_{n0}(t) \frac{\cosh[\lambda_{n0}(Z_i - H_i)]}{\cosh(\lambda_{n0} H_i)} + \frac{g}{R_i} c_{n0}(t) \right) \right. \\ & J_0(\lambda_{n0} R) - \frac{\sigma_i}{\rho_i R_i^3} c_{n0}(t) [Q_1 J_0''(\lambda_{n0} R) + \\ & Q_2 J_0'(\lambda_{n0} R)] \left. \right\} = (\dot{v}_z + \dot{\omega}_x R_{yi} - \dot{\omega}_y R_{xi}) Z_0 \end{aligned} \quad (33)$$

$$\begin{aligned} & \sum_{n=1}^{\infty} \left\{ \left(\dot{b}_{n1}(t) \frac{\cosh[\lambda_{n1}(Z_i - H_i)]}{\cosh(\lambda_{n1} H_i)} + \frac{g}{R_i} d_{n1}(t) \right) \right. \\ & J_1(\lambda_{n1} R) - \frac{\sigma_i}{\rho_i R_i^3} d_{n1}(t) [Q_1 J_1''(\lambda_{n1} R) + \\ & Q_2 J_1'(\lambda_{n1} R) - Q_3 J_1(\lambda_{n1} R)] \left. \right\} = \\ & - [\dot{v}_y + \dot{\omega}_z R_{xi} - \dot{\omega}_x (R_{zi} + Z_i)] R - \sum_{n=1}^{\infty} \end{aligned}$$

$$\left[\frac{4\dot{\omega}_x}{\lambda_{n1}(\lambda_{n1}^2 - 1)J_1(\lambda_{n1})} \frac{\sinh(\lambda_{n1}Z_i)}{\cosh(\lambda_{n1}H_i)} J_1(\lambda_{n1}R) \right] Q_3 = \frac{2}{R^2} \left(\frac{(1 - R^3)}{4 - 4R^3 + 9R^4\beta_i^2} \right)^{\frac{1}{2}}$$

(34)

$$\sum_{n=1}^{\infty} \left\{ \left(\dot{a}_{n1}(t) \frac{\cosh[\lambda_{n1}(Z_i - H_i)]}{\cosh(\lambda_{n1}H_i)} + \frac{g}{R_i} c_{n1}(t) \right) J_1(\lambda_{n1}R) - \frac{\sigma_i}{\rho_i R_i^3} c_{n1}(t) [Q_1 J_1''(\lambda_{n1}R) + Q_2 J_1'(\lambda_{n1}R) - Q_3 J_1(\lambda_{n1}R)] \right\} = \\ - [\dot{v}_x - \dot{\omega}_z R_{yi} + \dot{\omega}_y (R_{xi} + Z_i)] R + \sum_{n=1}^{\infty} \frac{4\dot{\omega}_y}{\lambda_{n1}(\lambda_{n1}^2 - 1)J_1(\lambda_{n1})} \frac{\sinh(\lambda_{n1}Z_i)}{\cosh(\lambda_{n1}H_i)} J_1(\lambda_{n1}R)$$

(35)

式中：

$$Q_1 = \left(\frac{4(1 - R^3)}{4 - 4R^3 + 9R^4\beta_i^2} \right)^{\frac{3}{2}}$$

$$Q_2 =$$

$$\frac{4(8 - 16R^3 + 8R^6 - 90R^4\beta_i^2 + 9R^7\beta_i^2)(1 - R^3)^{\frac{1}{2}}}{R(4 - 4R^3 + 9R^4\beta_i^2)^{\frac{5}{2}}}$$

$$\bar{A}_{ns} = \begin{cases} 2 \int_0^1 \left\{ -\frac{\lambda_{n0} \sinh[\lambda_{n0}(Z_i - H_i)]}{\cosh(\lambda_{n0}H_i)} J_0(\lambda_{n0}R) + \frac{\cosh[\lambda_{n0}(Z_i - H_i)]}{\cosh(\lambda_{n0}H_i)} [J_0(\lambda_{n0}R)]' \left(\frac{dF_i}{dR} \right) \right\} R dR, & s = 0 \\ \frac{2}{J_0^2(\lambda_{s0})} \int_0^1 \left\{ -\frac{\lambda_{n0} \sinh[\lambda_{n0}(Z_i - H_i)]}{\cosh(\lambda_{n0}H_i)} J_0(\lambda_{n0}R) + \frac{\cosh[\lambda_{n0}(Z_i - H_i)]}{\cosh(\lambda_{n0}H_i)} [J_0(\lambda_{n0}R)]' \left(\frac{dF_i}{dR} \right) J_0(\lambda_{s0}R) R dR, & s \neq 0 \end{cases}$$

$$\bar{B}_{ns} = \begin{cases} 2 \int_0^1 \frac{\cosh[\lambda_{n0}(Z_i - H_i)]}{\cosh(\lambda_{n0}H_i)} \cdot J_0(\lambda_{n0}R) R dR, & s = 0 \\ \frac{2}{J_0^2(\lambda_{s0})} \int_0^1 \frac{\cosh[\lambda_{n0}(Z_i - H_i)]}{\cosh(\lambda_{n0}H_i)} \cdot J_0(\lambda_{n0}R) J_0(\lambda_{s0}R) R dR, & s \neq 0 \end{cases}$$

$$\bar{C}_{ns} = \begin{cases} 2 \int_0^1 \left\{ \frac{g}{R_i} J_0(\lambda_{n0}R) - \frac{\sigma_i}{\rho_i R_i^3} \cdot [Q_1 J_0''(\lambda_{n0}R) + Q_2 J_0'(\lambda_{n0}R)] \right\} R dR, & s = 0 \\ \frac{2}{J_0^2(\lambda_{s0})} \int_0^1 \left\{ \frac{g}{R_i} J_0(\lambda_{n0}R) - \frac{\sigma_i}{\rho_i R_i^3} \cdot [Q_1 J_0''(\lambda_{n0}R) + Q_2 J_0'(\lambda_{n0}R)] \right\} J_0(\lambda_{s0}R) R dR, & s \neq 0 \end{cases}$$

$$\bar{P}_{ns} = \begin{cases} \bar{v}_z + \omega_x R_{yi} - \omega_y R_{xi}, & s = 0 \\ 0, & s \neq 0 \end{cases}$$

$$\bar{Q}_{ns} = \begin{cases} (\dot{v}_z + \dot{\omega}_x R_{yi} - \dot{\omega}_y R_{xi}) \cdot 2 \int_0^1 R_i \beta_i [1 - (1 - R^3)^2] R dR, & s = 0 \\ (\dot{v}_z + \dot{\omega}_x R_{yi} - \dot{\omega}_y R_{xi}) \frac{2}{J_0^2(\lambda_{s0})} \cdot \int_0^1 R_i \beta_i [1 - (1 - R^3)^2] J_0(\lambda_{s0}R) R dR, & s \neq 0 \end{cases}$$

依据式(30)~(35)可知,因航天器姿态和轨道坐标运动引发贮箱内液体耦合晃动稳态解的占优模态有:周向0阶对称模态($m = 0$)、周向1阶($m = 1$)对称模态(面内模态)和周向1阶($m = 1$)反对称模态(面外模态),这与前面仅当 $m = 0$ 和1时的晃动模态产生晃动力和晃动力矩的结论保持一致。下面将具体推导相对晃动速度势模态系数和晃动波高模态系数应满足的耦合晃动动力学状态方程。

(1) 关于周向0阶对称模态系数的状态方程

将式(30)、(33)同时利用式0阶贝赛尔函数在第二类边界条件下的级数展开式进行展开,并利用贝赛尔函数的正交性后,分别可得

$$\sum_{n=1}^N (\dot{c}_{n0} + \bar{A}_{ns} a_{n0}) = \bar{P}_s \quad (36)$$

$$\sum_{n=1}^N [\bar{B}_{ns} \dot{a}_{n0} + \bar{C}_{ns} c_{n0}] = \bar{Q}_s \quad (37)$$

式中: $s = 0, 1, 2, \dots, N$;方程中各系数表达式分别如下

由于式(36)、(37)中共有 $2N$ 个未知晃动模态系数,但有 $2N+2$ 个微分方程,故在计算应将 $s=0$ 的项作为边界条件处理后,将航天器主体的速度和角速度并入状态向量中。

(2) 关于周向1阶对称模态系数(一阶面内模态)的状态方程

利用一阶贝赛尔函数在第二类边界条件下的级数展开式对将式(31)、(34)进行展开后,分别可得

$$\sum_{n=1}^{\infty} \left\{ \dot{d}_{n1}(t) J_1(\lambda_{n1} R) - b_{n1}(t) \sum_{s=1}^{\infty} \bar{D}_{ns} J_1(\lambda_{s1} R) - \omega_x \sum_{s=1}^{\infty} \bar{E}_{ns} J_1(\lambda_{s1} R) + \omega_x \frac{2}{(\lambda_{n1}^2 - 1) J_1(\lambda_{n1})} \right. \\ \left. J_1(\lambda_{n1} R) \right\} = 0 \quad (38)$$

$$\sum_{n=1}^{\infty} \left\{ \dot{b}_{n1}(t) \bar{F}_{ns} J_1(\lambda_{s1} R) + \frac{g}{R_i} \dot{d}_{n1}(t) J_1(\lambda_{n1} R) - d_{n1}(t) \sum_{s=1}^{\infty} \bar{G}_{ns} J_1(\lambda_{s1} R) \right\} = - \sum_{n=1}^{\infty} \left[\dot{\omega}_x \sum_{s=1}^{\infty} \bar{H}_{ns} J_1(\lambda_{s1} R) \right] - (\dot{v}_y + \dot{\omega}_z R_{xi}) \sum_{n=1}^{\infty} \frac{2}{(\lambda_{n1}^2 - 1) J_1(\lambda_{n1})} \\ J_1(\lambda_{n1} R) + \dot{\omega}_x \sum_{n=1}^{\infty} \bar{I}_n J_1(\lambda_{n1} R) \quad (39)$$

式中:

$$\bar{D}_{ns} = \frac{2\lambda_{s1}^2}{(\lambda_{s1}^2 - 1) J_1^2(\lambda_{s1})} \int_0^1 \left\{ \frac{\lambda_{n1} \sinh[\lambda_{n1}(Z_i - H_i)]}{\cosh(\lambda_{n1} H_i)} \right. \\ \left. J_1(\lambda_{n1} R) - \frac{\cosh[\lambda_{n1}(Z_i - H_i)]}{\cosh(\lambda_{n1} H_i)} \right\}' \left(\frac{dF_i}{dR} \right) J_1(\lambda_{s1} R) R dR$$

$$\bar{E}_{ns} = \frac{2\lambda_{s1}^2}{(\lambda_{s1}^2 - 1) J_1^2(\lambda_{s1})} \int_0^1 \left\{ \frac{4}{(\lambda_{n1}^2 - 1) J_1(\lambda_{n1})} \right. \\ \left. \frac{\cosh(\lambda_{n1} Z_i)}{\cosh(\lambda_{n1} H_i)} J_1(\lambda_{n1} R) - \frac{4}{\lambda_{n1}(\lambda_{n1}^2 - 1) J_1(\lambda_{n1})} \right. \\ \left. \frac{\cosh(\lambda_{n1} Z_i)}{\cosh(\lambda_{n1} H_i)} [J_1(\lambda_{n1} R)]' \left(\frac{dF_i}{dR} \right) \right\}' \\ J_1(\lambda_{s1} R) R dR ;$$

$$\bar{F}_{ns} = \frac{2\lambda_{s1}^2}{(\lambda_{s1}^2 - 1) J_1^2(\lambda_{s1})} \int_0^1 \frac{\cosh[\lambda_{n1}(Z_i - H_i)]}{\cosh(\lambda_{n1} H_i)}$$

$$J_1(\lambda_{n1} R) J_1(\lambda_{s1} R) R dR$$

$$\bar{G}_{ns} = \frac{2\lambda_{s1}^2}{(\lambda_{s1}^2 - 1) J_1^2(\lambda_{s1})} \int_0^1 \frac{\sigma_i}{\rho_i R_i^3} [Q_1 J_1''(\lambda_{n1} R) + Q_2 J_1'(\lambda_{n1} R) - Q_3 J_1(\lambda_{n1} R)] J_1(\lambda_{s1} R) R dR$$

$$\bar{H}_{ns} = \frac{2\lambda_{s1}^2}{(\lambda_{s1}^2 - 1) J_1^2(\lambda_{s1})} \int_0^1 \frac{4 J_1(\lambda_{n1} R)}{\lambda_{n1}(\lambda_{n1}^2 - 1) J_1(\lambda_{n1})} \cdot \frac{\sinh(\lambda_{n1} Z_i)}{\cosh(\lambda_{n1} H_i)} J_1(\lambda_{s1} R) R dR$$

$$\bar{I}_n = \frac{2\lambda_{s1}^2}{(\lambda_{s1}^2 - 1) J_1^2(\lambda_{s1})} \int_0^1 (R_{zi} + Z_i) J_1(\lambda_{s1} R) R^2 dR$$

利用Bessel函数的正交性,由式(38)、(39)分别可得

$$\dot{d}_{n1}(t) - \sum_{s=1}^{\infty} b_{s1}(t) \bar{D}_{sn} = \omega_x \sum_{s=1}^{\infty} \bar{E}_{sn} - \frac{2\omega_x}{(\lambda_{n1}^2 - 1) J_1(\lambda_{n1})} \quad (40)$$

$$\sum_{s=1}^{\infty} \dot{b}_{s1}(t) \bar{F}_{sn} + \frac{g}{R_i} \dot{d}_{n1}(t) - \sum_{s=1}^{\infty} d_{s1}(t) \bar{G}_{sn} = - \dot{\omega}_x \sum_{s=1}^{\infty} \bar{H}_{sn} - \frac{2(\dot{v}_y + \dot{\omega}_z R_{xi})}{(\lambda_{n1}^2 - 1) J_1(\lambda_{n1})} + \bar{I}_n \dot{\omega}_x \quad (41)$$

(3) 关于周向1阶反对称模态系数(一阶面外模态)的状态方程

同理,依据式(32)、(35)分别可得

$$\dot{c}_{n1}(t) - \sum_{s=1}^{\infty} a_{s1}(t) \bar{D}_{sn} = - \omega_y \sum_{s=1}^{\infty} \bar{E}_{sn} + \frac{2\omega_y}{(\lambda_{n1}^2 - 1) J_1(\lambda_{n1})} \quad (42)$$

$$\sum_{s=1}^{\infty} \dot{a}_{s1}(t) \bar{F}_{sn} + \frac{g}{R_0} c_{n1}(t) - \sum_{s=1}^{\infty} c_{s1}(t) \bar{G}_{sn} = \bar{I}_{n1} \dot{\omega}_y - \frac{2(\dot{v}_x + \dot{\omega}_z R_{yi})}{(\lambda_{n1}^2 - 1) J_1(\lambda_{n1})} + \dot{\omega}_y \sum_{s=1}^{\infty} \bar{H}_{sn} \quad (43)$$

1.6 航天器主体的动力学状态方程

取主刚体的主惯性轴为其本体坐标系,若忽略势能的影响,主刚体的拉格朗日函数可写为

$$L = \frac{1}{2} m_0 \mathbf{v}^T \mathbf{v} + \frac{1}{2} \boldsymbol{\omega}^T J \boldsymbol{\omega} \quad (44)$$

式中: m_0 为主刚体质量; J 为主刚体转动惯量。

对主刚体采用准坐标系下的拉格朗日方程建立动力学方程,其形式如下^[17]

$$\begin{cases} \frac{d}{dt} \left\{ \frac{\partial L}{\partial V} \right\} + \boldsymbol{\omega}^* \left\{ \frac{\partial L}{\partial V} \right\} - \mathbf{C}_0 \left\{ \frac{\partial L}{\partial R} \right\} = \mathbf{F}_0 + \sum_{i=1}^{I_{\text{tank}}} \mathbf{F}_{\text{shock}} \\ \frac{d}{dt} \left\{ \frac{\partial L}{\partial \boldsymbol{\omega}} \right\} + v^* \left\{ \frac{\partial L}{\partial V} \right\} + \boldsymbol{\omega}^* \left\{ \frac{\partial L}{\partial \boldsymbol{\omega}} \right\} - \\ (\mathbf{D}_0^T)^{-1} \left\{ \frac{\partial L}{\partial \theta} \right\} = \mathbf{M}_0 + \sum_{i=1}^{I_{\text{tank}}} \mathbf{M}_{\text{shock}} \end{cases} \quad (45)$$

式中: I_{tank} 为充液圆柱贮箱的个数; \mathbf{F}_0 、 \mathbf{M}_0 分别为作用在航天器主体上沿本体坐标轴的非保守外力和非保守外力矩;

$$\begin{aligned} \mathbf{F}_{\text{shock}} &= [F_{xi}(t), F_{yi}(t), F_{zi}(t)]^T \\ \mathbf{M}_{\text{shock}} &= [M_{xi}(t), M_{yi}(t), 0]^T \end{aligned}$$

1.7 航天器整体系统的刚 - 液耦合动力学状态方程

联立式(36)~(43)、(45), 并将式(21)~(23)、(26)~(27)代入后, 最终可得航天器整体系统的动力学状态方程, 其矩阵形式如下

$$\tilde{\mathbf{M}}(\tilde{\mathbf{Z}}, t) \frac{d\tilde{\mathbf{Z}}}{dt} = \mathbf{H}(\tilde{\mathbf{Z}}, t) + \tilde{\mathbf{F}} \quad (46)$$

式中: $\tilde{\mathbf{Z}}$ 为整体系统的状态向量, 其包含所有贮箱的晃动速度势系数、晃动波高系数、航天器主体轨道坐标及速度、姿态角及角速度, 共 $(6N \cdot I_{\text{tank}} + 12)$ 个变量; $\tilde{\mathbf{M}}(\tilde{\mathbf{Z}}, t)$ 为时变的非奇异的广义质量矩阵, 由于篇幅有限, 文中就不详细赘述其具体的表达式。另外, 运用四阶龙格 - 库塔法对式(46)进行了求解, 并编制出适用于带多充液柱贮航天器内刚 - 液耦合动力计算的模块化计算程序, 其中程序流程图如图 2 所示。

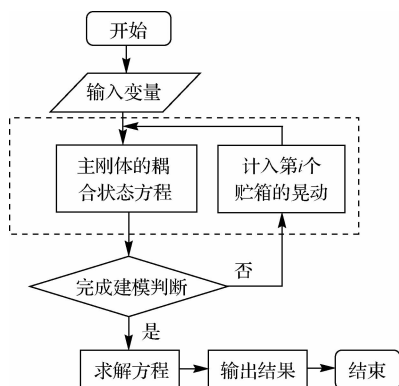


图 2 刚 - 液耦合计算程序流程图

Fig. 2 Program flow chart of Rigid-liquid coupled computing

2 算例仿真

航天器主体、液体燃料及贮箱的主要参数分别

为: $m_0 = 800 \text{ kg}$; $J_{xx} = J_{yy} = J_{zz} = 1500 \text{ kg} \cdot \text{m}^2$; $\sigma = 3.39 \times 10^{-2} \text{ N} \cdot \text{m}^{-1}$; $\rho = 0.86 \times 10^3 \text{ kg} \cdot \text{m}^{-3}$; $g = 9.8 \times 10^{-2} \text{ N} \cdot \text{m}^{-2}$ 。为研究多贮耦合晃动对航天器姿态和轨道的影响, 文中考虑了贮箱分别在 oxy 平面内按图 3 所示四种情况进行布置, 图中: $R_1 = 0.6 \text{ m}$; $R_2 = 0.4 \text{ m}$; $R_3 = 0.3 \text{ m}$, $d_1 = 1.2 \text{ m}$, $d_2 = 0.2 \text{ m}$, $d_3 = 0.8 \text{ m}$, 并联贮箱沿 oz 轴仅布置一列, 且 oxy 平面位于充液深度中心点处。

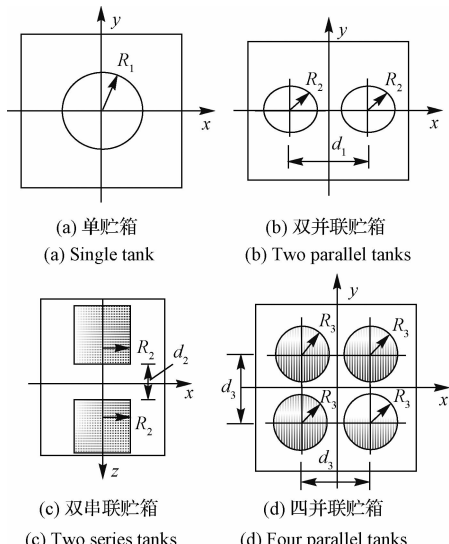


图 3 不同的贮箱分布情况

Fig. 3 Difference layouts of tanks

在航天器携带的液体总质量保持不变的情况下, 不同尺寸贮箱的固有频率随液体总质量的变化曲线如图 4 所示。

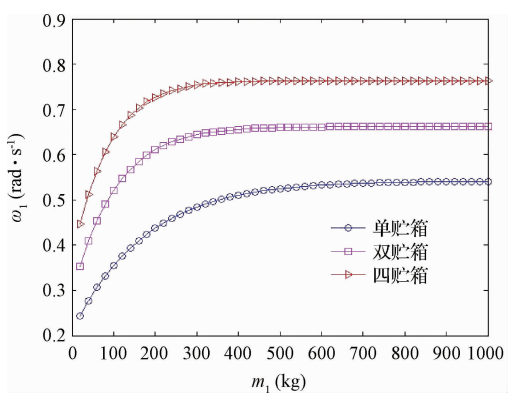


图 4 一阶固有频率随液体总质量的变化曲线

Fig. 4 Curves of first natural frequency vs. liquid total mass

由图 4 可知, 贮箱尺寸和充液深度对液体晃动的一阶固有频率影响比较明显, 当航天器中液体燃料足够多时, 贮箱内液体晃动的固有频率趋于稳定,

这将有利于航天器控制系统稳定性的分析与设计;但随着航天器中液体燃料的大量消耗,贮箱内液体晃动的固有频率变化较大,尤其对携带多充液贮箱的航天器而言,如出现各贮箱内的燃料消耗不均匀,这在航天器的设计中,将会对航天器系统动态特性的预测产生一定的困难,从而更加增大对航天器控制系统的效率和稳定性问题计算的难度。以双并联贮箱为例,图5~7给出了受外界干扰后,两贮箱内具有几种不同充液深度时,液体自由晃动波高和航天器姿态角的变化曲线。

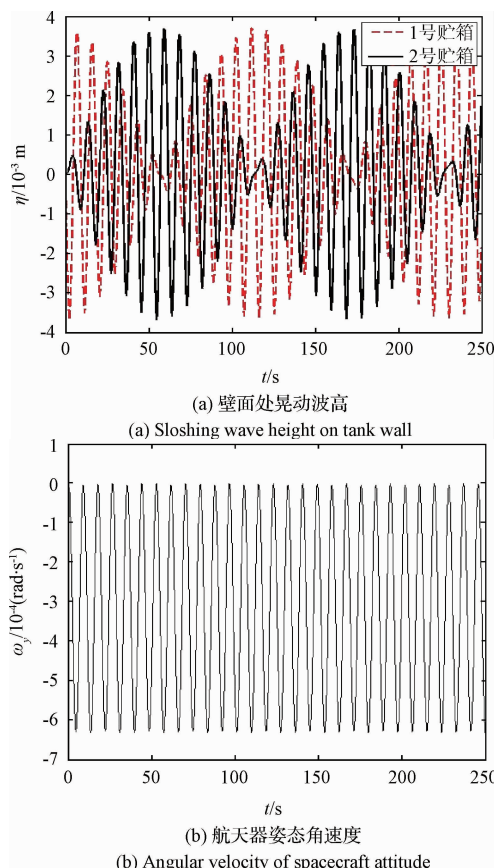


图5 当 $h_2 = h_1 = 0.694$ m 时的响应

Fig.5 The responses when $h_2 = h_1 = 0.694$ m

通过对图5~7可知,在带多充液贮箱航天器的计算设计中,应尽量减少不同贮箱内燃料消耗的不均匀性。另外,为研究航天器的驱动方式对航天器刚-液耦合系统的影响,设驱动力或驱动力矩分别按图8所示两种具有相同冲量的不同类型的驱动力作用于航天器主体上。

当驱动力为沿主体坐标系ox轴的横向驱动力时,航天器刚-液耦合系统的响应分别如图9~10

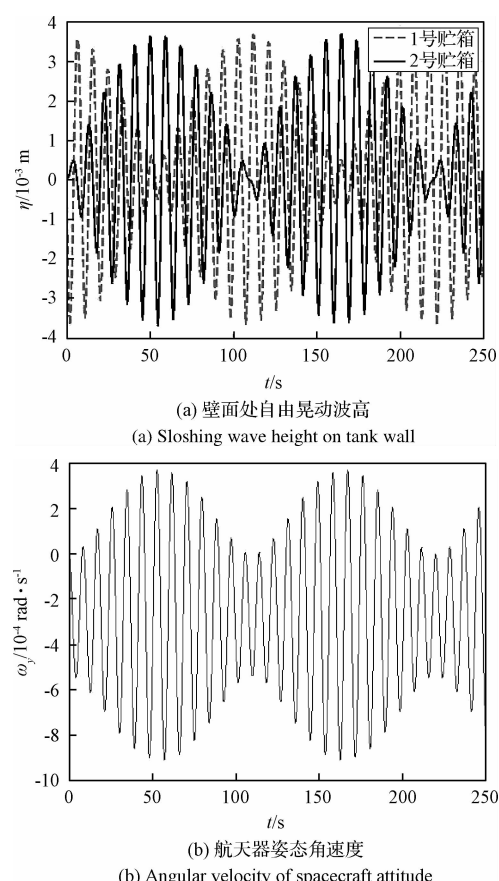


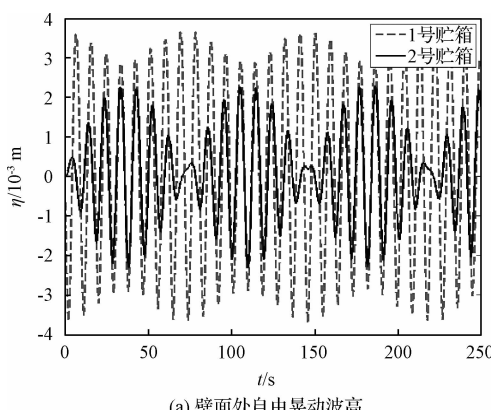
图6 当 $h_2 = 0.6h_1 = 0.4164$ m 时的响应

Fig.6 The responses when $h_2 = 0.6h_1 = 0.4164$ m

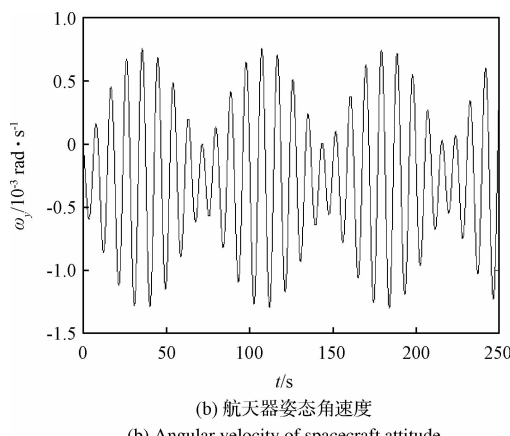
所示,其中,取 $(F_x)_{\max} = 10$ N。

由图9~10可知,带多小尺寸充液贮箱航天器在受驱动力作用时的快速响应、姿态角的影响和晃动幅值的大小等方面的动态性能均优于带单大尺寸贮箱航天器的性能,且在保持携带的燃料总质量不变的前提下,随着贮箱数量的增多,航天器的上述动态性能均变得越来越有利于航天器姿态、轨道的控制与稳定。当然,如要更全面的了解带多充液贮箱航天器的各项动力学性能及优缺点,应依据实际工程的需求,综合分析航天器在各种不同工况下的各项性能后才能进行更具说服力的评估。

虽然,采用上述两种不同驱动方式时,充液航天器刚-液耦合系统的部分动态性能的变化趋势容易预测,但正因如此,才能够从侧面上反映出文中计算方法和所编程序的正确性和可靠性,为进一步的研究打下一定的理论基础。



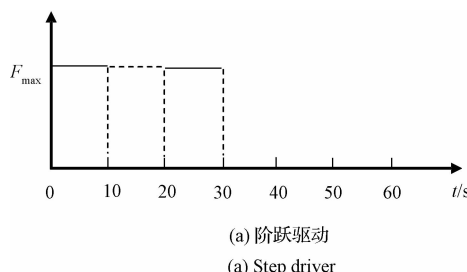
(a) 壁面处自由晃动波高
(a) Sloshing wave height on tank wall



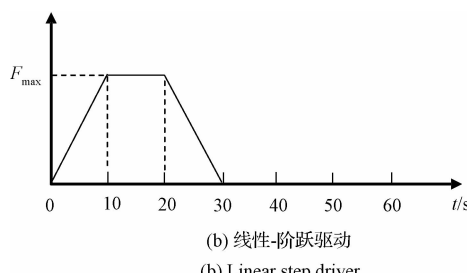
(b) 航天器姿态角速度
(b) Angular velocity of spacecraft attitude

图 7 当 $h_2 = 0.3h_1 = 0.208$ m 时的响应

Fig. 7 The responses when $h_2 = 0.3h_1 = 0.208$ m



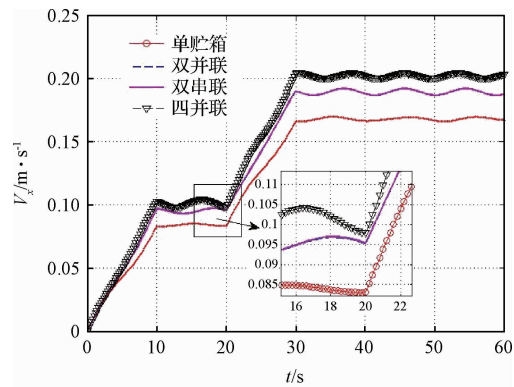
(a) 阶跃驱动
(a) Step driver



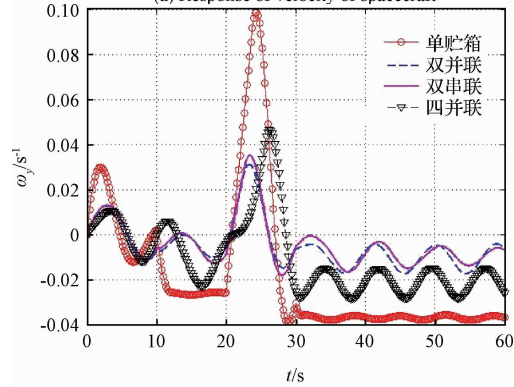
(b) 线性-阶跃驱动
(b) Linear step driver

图 8 不同的驱动方式

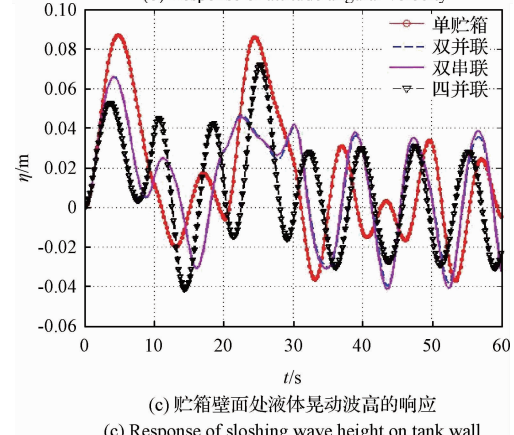
Fig. 8 Difference types of drivers



(a) 航天器速度的响应
(a) Response of velocity of spacecraft



(b) 姿态角速度的响应
(b) Response of attitude angular velocity



(c) 贮箱壁面处液体晃动波高的响应
(c) Response of sloshing wave height on tank wall

图 9 航天器在横向阶跃驱动力下的计算结果

Fig. 9 Results when spacecraft under step driver

3 结论与展望

文中直接以贮箱内液体晃动速度模态系数、晃动波高模态系数和航天器姿、轨坐标等参数为未知状态变量, 较系统地得到了带多充液贮箱刚性航天器刚-液耦合系统动力学问题求解的一种半解析法, 为从理论上了解该类航天器的动力学本质和实际工程设计与应用提供一定的理论指导。但文中文

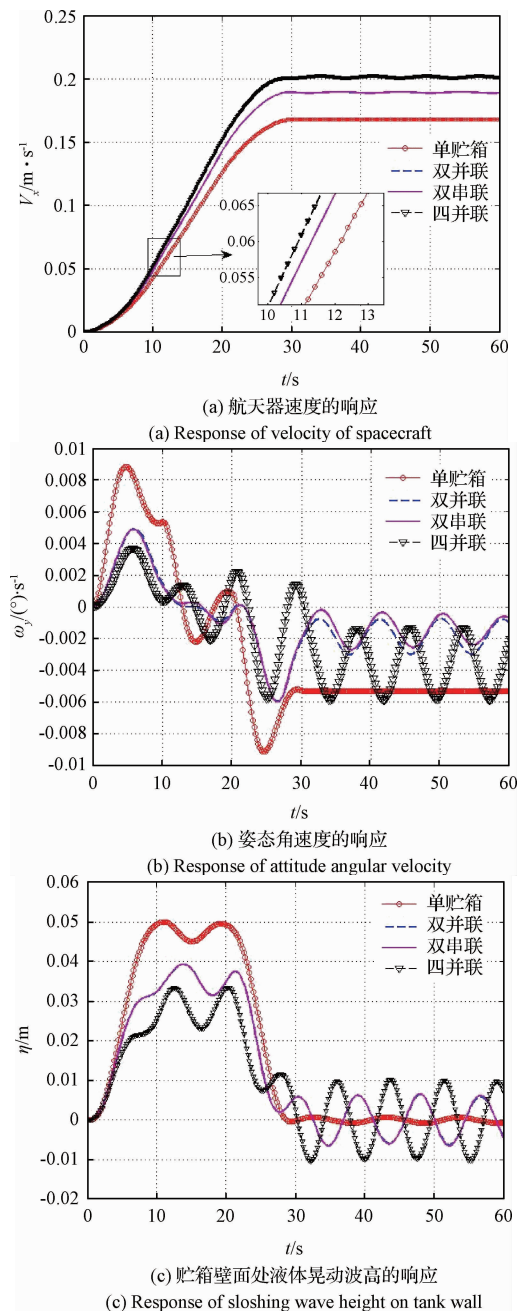


图 10 航天器在横向线性阶跃驱动力下的计算结果

Fig. 10 Results when spacecraft under linear step driver

法相对于工程实际应用的需求来讲,仍有许多不足之处有待改进,例如:文中方法仅限于对线性晃动情况下小幅姿态角干扰的刚 - 液耦合问题进行研究,对于大幅姿态角干扰时,需进一步研究大角度偏置贮箱内液体晃动的求解。

参 考 文 献

- [1] Marthinus C S. The coupled nonlinear dynamics of spacecraft with fluids in tanks of arbitrary geometry [D]. Cambridge:

- Massachusetts Institute of Technology, 1989.
- [2] Peterson L D, Crawley E F, Hansman R J. Nonlinear fluid slosh coupled to the dynamics of spacecraft [J]. AIAA Journal, 1989, 27(9):1230 - 1240.
- [3] Hung R J, Long Y T, Chi Y M. Slosh dynamics coupled with spacecraft attitude dynamics part 1: formulation and theory [J]. Journal of Spacecraft and Rockets, 1996, 33(4): 575 - 581.
- [4] Hung R J, Long Y T, Chi Y M. Slosh dynamics coupled with spacecraft attitude dynamics part 2: orbital environment application [J]. Journal of Spacecraft and Rockets, 1996, 33(4): 582 - 593.
- [5] Yue B Z. Study on the chaotic dynamics in attitude maneuver of liquid-filled flexible spacecraft [J]. AIAA Journal, 2011, 49(10): 2090 - 2099.
- [6] Shageer H, Tao G. Zero dynamics analysis for spacecraft with fuel slosh [C]. AIAA Guidance, Navigation, and Control Conference and Exhibit, Honolulu, August 18 - 21, 2008.
- [7] Sabri F, Lakis A A. Effects of sloshing on flutter prediction of partially liquid-filled circular cylindrical shell [J]. Journal of Aircraft, 2011, 48(6): 1829 - 1839.
- [8] 贾英宏,徐世杰.充液挠性多体航天器的变结构控制[J].宇航学报,2002,23(3):18 - 23. [Jia Ying-hong, Xu Shi-jie. Variable structure control for liquid-filled flexible multi-body spacecraft [J]. Journal of Astronautics, 2002, 23(3): 18 - 23.]
- [9] Kang J Y, Lee S. Attitude acquisition of a satellite with a partially filled liquid tank [J]. Journal of Guidance, Control and Dynamics, 2008, 31(3): 790 - 793.
- [10] 黄华,曲广吉.带多个充液储箱航天器的耦合动力学建模方法[J].空间控制技术与应用,2010, 36(3):14 - 19. [Huang Hua, Qu Guang-ji. Coupled Dynamics modeling of liquid sloshing for spacecraft with multiple propellant tanks [J]. Aerospace Control and Application, 2010, 36(3):14 - 19.]
- [11] Paul M, Scott R S. The effects of propellant slosh dynamics on the solar dynamics observatory [C]. AIAA Guidance, Navigation, and Control Conference, Oregon, August 08 - 11, 2011.
- [12] 岳宝增,祝乐梅.携带晃动燃料柔性航天器姿态机动中的同宿环分叉研究[J].宇航学报,2011,32(5): 991 - 997. [Yue Bao-zeng, Zhu Le-mei. Heteroclinic Bifurcations in Attitude Maneuver of Slosh-Coupled Spacecraft with Flexible Appendage [J]. Journal of Astronautics, 2011, 32(5): 991 - 997.]
- [13] Reyhanoglu M, Hervas J R. Nonlinear dynamics and control of space vehicles with multiple fuel slosh modes [J]. Control Engineering Practice, 2012, 20(9): 912 - 918.
- [14] Yue B Z, Zhu L M. Hybrid control of liquid-filled spacecraft maneuvers by dynamic inversion and input shaping [J]. AIAA Journal, 2014, 52(3): 618 - 626.
- [15] 吴文军,岳宝增.低重环境下圆柱贮箱内液体晃动特性研究

的一种解析法 [J]. 宇航学报, 2014, 35(4) : 397 – 406. [Wu Wen-jun, Yue Bao-zeng. An analytical method for studying the sloshing properties of liquid in cylindrical tank under low gravity environment [J]. Journal of Astronautics, 2014, 35(4) :397 – 406.]

- [16] 吴文军, 岳宝增. 低重环境下俯仰运动圆柱贮箱内液体晃动 [J]. 力学学报, 2014, 46(2) :284 – 290. [Wu Wen-jun, Yue Bao-zeng. Low-gravity liquid sloshing in cylindrical tanks under pitching excitation [J]. Chinese Journal of Theoretical and Applied Mechanics, 2014 , 46(2) :284 – 290.]

- [17] Meirovitch L. Methods of analytical dynamics [M], New York, McGraw-Hill, 1970.

作者简介:

吴文军(1982 -),男,讲师,博士研究生,主要从事航天器姿态稳定与控制、复杂结构动力学分析与振动控制仿真等方面的研究。

岳宝增(1962-),男,教授,博士生导师,主要从事非线性动力学与控制、液体非线性晃动力学及航天器动力学与控制等方面的研究。

通信地址:北京海淀区中关村南大街 5 号北京理工大学宇航学院(100081)

电话:13693289762

E-mail:bzyue@bit.edu.cn

(编辑:张宇平)